the central atom also provides the explanation of why the heptacoordinated main group fluorides prefer pentagonal-bipyramidal structures and not the monocapped octahedral or trigonal prismatic ones expected from VSEPR arguments.[63]

The possible puckering of the equatorial plane in pentagonal-bipyramidal molecules is due to the high degree of congestion in this plane. While in XeF_5^- (r(Xe–F) ≈ 2.00 Å)[4] the congestion is relatively low and, therefore, the anion is still planar, the considerably shorter equatorial I–F bonds (r = 1.857 Å)[5] in IF_7 result in increased repulsion and significant puckering.

Conclusion

The problems previously encountered with the vibrational spectra and normal coordinate analyses of IF_7 have been resolved and were caused by partially incorrect assignments. It is shown that the lowest energy structure of IF_7 is a pentagonal bipyramid of D_{5h} symmetry that can undergo a facile, rapid, dynamic, low-frequency equatorial ring puckering with very large vibrational amplitudes. Equivalence of the five equatorial ligands in species of five-fold symmetry is most likely achieved by Bartell's pseudorotational mechanism,[5] which can also account for the deviations from D_{5h} symmetry observed by electron diffraction studies of the molecules at room temperature in the gas phase. The pentagonal-bipyramidal structures of heptacoordinated fluoride or oxyfluoride complexes, the planarity of their equatorial ligands in their minimum-energy structures, and the large differences in their equatorial and axial bond lengths are attributed to a bonding scheme which involves a planar, delocalized $P_{x,y}$ hybrid orbital of the cental atom for the formation of five equatorial, semi-ionic, 6-center 10-electron bonds and an sp_z hybrid for the formation of two mainly covalent axial bonds. The apparent puckering of the fluorine ligands in the equatorial plane is due to their wide vibrational amplitudes involving large vibrational quantum numbers. This effect depends strongly on the relative sizes of the central atom and its ligands and the temperature. Thus, XeF_5^-, which is least congested, is, within experimental error, planar,[4] while IF_6O^- is strongly puckered, but its degree of puckering significantly decreases with decreasing temperature.[62] In IF_7, the I–F bonds are the shortest and, hence, the puckering is most pronounced. These data suggest that a wide spectrum of structures should exist for pentagonal-bipyramidal molecules which range from complete planarity to a strong puckering of the equatorial ligands.

Acknowledgment. The authors thank Drs. H. Oberhammer, L. Bartell, C. J. Schack, W. W. Wilson, and R. D. Wilson for helpful discussions and the Air Force Phillips Laboratory and the U.S. Army Research Office for financial support of the work carried out at Rocketdyne. We also thank Dr. Oberhammer for a copy of his program for the calculation of mean square amplitudes of vibration.

Note Added in Proof: The Coriolis ζ constants of the E_1' block of IF_7 were calculated from the force field and have the following values: $\zeta_{55} = -0.113$, $\zeta_{66} = 0.201$, $\zeta_{77} = 0.913$. Using these values, Dr. L. Bernstein has calculated the infrared band contour of ν_5. It exhibits a PQR structure similar to that observed for the 670 cm^{-1} band. The absence of pronounced PQR structure for the 746-cm^{-1} band is attributed to interference from hot bands. A high resolution study would be required to better understand the details of the observed band contours.

Molecular Dynamics Simulation of the Hydrated d(CGCGAATTCGCG)$_2$ Dodecamer

Karol Miaskiewicz,† Roman Osman,* and Harel Weinstein

Contribution from the Department of Physiology and Biophysics, Mount Sinai School of Medicine, New York, New York 10029. *Received July 24, 1992*

Abstract: A 150-ps MD simulation of the DNA dodecamer d(CGCGAATTCGCG)$_2$ surrounded by 22 sodium counterions and 1431 water molecules was performed with the AMBER force field. The trajectory of the simulation shows that the DNA structure was stable in the first 60 ps, it changed continuously in the interval 60–100 ps, and it stabilized again in the interval 100–150 ps. The structure was analyzed in the two time periods of simulation, 20–60 and 100–150 ps, in which the structure fluctuated around a stable average. The averaged DNA structure in the 100–150 ps of the simulation is highly distorted. Kinks are observed near the C3,G4 and C9,G10 residues. The helix is significantly unwound in the central AATT region. The base pairing and stacking interactions are also disturbed. The analysis of the trajectories of the counterions shows that they are quite mobile. They distribute equally between two types of configurations: in one the Na^+ reside in a direct coordination with the phosphate group, in the other the coordination to the phosphate is through a hydration sphere. The water molecules distribute in two solvation domains. The first solvation domain is very stable during the dynamics, while the rest undergoes a small expansion. The main hydration site in DNA is the phosphate group. The average number of water molecules hydrating a G–C base pair is 21.38, while the A–T pair is solvated by an average of 20.45 water molecules. The results raise the question whether a longer MD simulation would result in a "unique" stable structure of DNA.

Introduction

Early information on DNA structure was obtained from diffraction studies of oriented high molecular weight fibers.[1] The two basic families of DNA structures that were derived from these data are the A-DNA and the B-DNA. However, subsequent single crystal X-ray studies have shown that DNA structure is not uniform and shows many sequence dependent features. Sequence dependence of structure was especially well established for the d(CGCGAATTCGCG)$_2$ dodecamer by Dickerson et al.[2,3] Also, models have been proposed for sequence specific local deformations of the DNA double helix such as Calladine purine–purine clash[4] or the Trifonov wedge.[5,6] Recent crystallographic studies have

† Present address: Battelle, Pacific Northwest Laboratories, Richland, WA 99352.

(1) Franklin, R. E.; Gosling, R. G. *Acta Crystallogr.* **1953**, *6*, 673.
(2) Dickerson, R. E. *J. Mol. Biol.* **1981**, *149*, 761–786.
(3) Dickerson, R. E. *J. Mol. Biol.* **1983**, *166*, 419–441.
(4) Calladine, C. R. *J. Mol. Biol.* **1982**, *161*, 343–352.
(5) Trifonov, E. N.; Sussman, J. L. *Proc. Natl. Acad. Sci. U.S.A.* **1980**, *77*, 3816–3820.

0002-7863/93/1515-1526$04.00/0

also shown that the structure of DNA in crystals is highly sensitive to environmental effects including hydration, crystal packing, and temperature.[7,8] Thus, the structure of DNA, especially B-DNA, emerges as highly inhomogeneous and variable. In contrast, the A-DNA family shows less structural diversity than B-DNA.

DNA flexibility can be expected to be even more evident in solution than in the crystal. A considerable amount of structural data on polynucleotides in solution has been collected using CD, Raman, and NMR spectroscopic techniques, but the precision of structure determination with these techniques is model dependent and rather low. In CD studies, the spectrum of the polynucleotide is compared to standard spectra of sequences assumed to exist in well defined A- or B-DNA-like structures. On the basis of such comparisons the studied sequence is assigned to a specific structural class (usually either the A- or the B-DNA family). More detailed descriptions of DNA structure can be deduced from NMR spectra. Two-dimensional (2D) NMR techniques provide data on interproton distances, which are used as constraints in distance geometry calculations or in combination with restrained molecular dynamics. In the latter computational simulations, an effective potential representing experimental interproton distance is used to produce information on time-averaged structure of DNA in solution. Attempts to determine the backbone torsion angles from NMR spectra using proton–phosphorus coupling constants[9,10] have yielded polynucleotide structures that are equivalent to low resolution structures. Recently, it was shown that many different DNA conformations covering a wide range of torsional backbone angles can be fitted to the same data set of NMR distance restraints.[11] In some studies, different constraints on backbone torsional angles have even been assumed to produce a reasonable fit to experimental data.[12,13]

The large diversity of DNA structures in solution obtained thus far from experimental studies suggests a complexity that is not well understood. First, the structure of a specified DNA sequence could be very different in solution compared to that observed in the crystal. For example, the structure of the octamer d-(GGTATACC)$_2$ has been determined in solution as B-DNA for the GG/CC base pairs and as D-DNA-like in the central TATA/ATAT part.[14,15] However, an A-DNA structure has been found for this octamer in the crystal.[16] Also, the DNA binding site of transcription factor IIIA (TFIIIA) has been shown to have different structures in solution and in the crystal.[17] The DNA conformations obtained in solution are very different from the classic A- and B-DNA families and can hardly be described as belonging to one of these structural categories. Such structures are sometimes classified as an intermediate type, between the A- and B-forms of DNA.[18] Thus, some common features have been observed in the structures of d(GCATGC)$_2$, d(CTGGATCCAG)$_2$, and d(CGCGPATTCGCG)$_2$ (P stands for purine) in solution.[13] The most common feature is the behavior of CpG sequences, which show values of slide and roll characteristic for A-DNA, A-like interstrand stacking of the purines as well as a decrease in helical twist. Consequently, DNA is kinked at the CpG sequences in spite of the fact that the glycosidic and backbone torsion angles lie in the range characteristic for B-DNA. The observed conformations in solution are highly distorted and show a big variation of helical twist. For example, in the 14-mer d(CGCGTCGCGCGAGCG)$_2$ the base pairs are tilted and displaced from the helix axis.[19] A large roll angle opening the bases into the minor groove and a loss of stacking between bases are also observed in some segments of the 14-mer. In the NMR study of the solution structure of a 12-mer d(GGCGGAGTTAGG)·(CCTAACTCCGCC) such structural deviations as unusual sugar geometries, large propeller twisting, kinks, and unusual chemical shifts of some protons have been characterized.[20] Further evidence for a distorted structure comes from a flow linear dichroism study, which showed that in sequences believed to be in the B-DNA form, the largest angle that the bases can make with the helix axis is 73°.[21] DNA structures in solution are also intrinsically bent as suggested on the basis of electrophoretic mobility studies.[22,23]

These observations disagree with the common assumption that DNA in solution can be described as a single conformation. That the conformation of DNA is subject to dynamic changes is also suggested by the observation that polar hydrogens of the bases in DNA exchange with solvent hydrogens quite rapidly. This behavior has led to the suggestion that ordered helices contain small amounts of open states, covering about 10 adjacent base pairs, which can propagate along the helix.[24] The internal motion characterized as a rapid conformational equilibrium between unspecified states has been suggested as an explanation of NMR signal broadening observed for the 12-mer d(GGCGGAGTT-AGG)·d(CCTAACTCCGCC).[20] Some NMR data have been also interpreted in terms of an equilibrium between different sugar puckering states.[9] The known correlation between sugar puckering, the backbone torsional angle δ, and the glycosidic angle χ implies that dynamic changes in sugar pucker states lead to an interdependent dynamics of backbone conformations.

Several computational simulations of polynucleotide structures with the methods of molecular dynamics (MD)[25-32] have been reported recently. These calculations usually attempt to model the situation in solution by a distance dependent dielectric constant ($\epsilon = r$), but in some studies water molecules were included explicitly with[27] or without periodic boundary conditions.[25,29] Like the results from experimental studies in solution, the MD studies have yielded structures that do not belong strictly to either A-DNA or B-DNA. Bends and kinks were observed in the DNA helix, and both the base pairing and the stacking were found to be distorted. Although it is impossible to say that the simulated structures are in full agreement with those observed from experiments, they are not inconsistent with the available experimental observations on DNA structure in solutions.

Two 100-ps MD simulations of the dodecamer (CGCGAATTCGCG)$_2$ have been published recently.[30,31] In both simulations, aqueous solvent was modeled with a distance dependent dielectric constant. Among the structural details that

(6) Trifonov, E. N. *Nucl. Acids Res.* **1980**, *8*, 4041–4053.
(7) Jain, S.; Sundaralingam, M. *J. Biol. Chem.* **1989**, *264*, 12780–12784.
(8) Shakked, Z.; Guerstein-Guzikevich, G.; Eisenstein, M.; Frolow, F.; Rabinovich, D. *Nature* **1989**, *342*, 456–460.
(9) Schmitz, U.; Zon, G.; James, T. L. *Biochemistry* **1990**, *29*, 2357–2368.
(10) Powers, R.; Jones, C. R.; Gorenstein, D. G. *J. Biomol. Struct. Dyn.* **1990**, *8*, 253–294.
(11) Metzler, W. J.; Wang, C.; Kitchen, D. B.; Levy, R. M.; Pardi, A. *J. Mol. Biol.* **1990**, *214*, 711–736.
(12) Gronenborn, A. M.; Clore, G. M. *Biochemistry* **1989**, *28*, 5978–5984.
(13) Clore, G. M.; Oschkinat, H.; Mclaughlin, L. W.; Benseler, F.; Happ, C. S.; Happ, E.; Gronenborn, A. M. *Biochemistry* **1988**, *27*, 4185–4197.
(14) Jamin, N.; James, T. L. *Eur. J. Biochem.* **1985**, *152*, 157–166.
(15) Zhou, N.; Bianucci, A. M.; Pattabiraman, N.; James, T. L. *Biochemistry* **1987**, *26*, 7905–7913.
(16) Shakked, Z.; Rabinovich, D.; Kennard, O.; Cruse, W. B. T.; Salisbury, S. A.; Viswamitra, M. A. *J. Mol. Biol.* **1983**, *166*, 183–201.
(17) Gottesfeld, J. M.; Blanco, J.; Tennant, L. L. *Nature* **1987**, *329*, 460–462.
(18) Fairall, L.; Martin, S.; Rhodes, D. *EMBO J.* **1989**, *8*, 1809–1817.
(19) Patel, D. J.; Shapiro, L.; Hare, D. In *Unusual DNA Structures*; Wells, R. D., Harvey, S. C., Ed.; Springer-Verlag: New York, 1988; pp 115–161.
(20) Hsiung Lin, C.; Hill, G. C.; Hurley, L. H. *Chem. Res. Toxicol.* **1992**, 167–182.
(21) Dougherty, A. M.; Causley, G. C.; Johnson, C. W., Jr. *Proc. Natl. Acad. Sci. U.S.A.* **1983**, *80*, 2193–2195.
(22) Trifonov, E. N.; Ulanovsky, L. E. In *Unusual DNA Structures*; Wells, R. D., Harvey, S. C., Ed.; Springer-Verlag: New York, 1988; pp 173–187.
(23) Calladine, C. R.; Drew, H. R.; McCall, M. J. *J. Mol. Biol.* **1988**, *201*, 127–137.
(24) Englander, S. W.; Kallenbach, N. R.; Heeger, A. J.; Krumhansl, J. A.; Litwin, S. *Proc. Natl. Acad. Sci. U.S.A.* **1980**, *77*, 7222–7226.
(25) Seibel, G. L.; Singh, U. C.; Kollman, A. P. *Proc. Natl. Acad. Sci. U.S.A.* **1985**, *82*, 6537–6540.
(26) Singh, U. C.; Weiner, S. T.; Kollman, P. *Proc. Natl. Acad. Sci. U.S.A.* **1985**, *82*, 755–759.
(27) van Gunsteren, W. F.; Berendsen, H. J. C.; Geurtsen, R. G.; Zwinderman, H. R. J. *Ann. N.Y. Acad. Sci.* **1986**, *482*, 287–303.
(28) Zielinski, T. J.; Shibata, M.; Reine, R. *Febs.* (*Fed. Eur. Biochem. Soc.*) *Lett.* **1988**, *236*, 450–454.
(29) Zielinski, T. J.; Shibata, M. *Biopolymers* **1990**, *29*, 1027–1044.
(30) Srinivasan, J.; Withka, J. W.; Beveridge, D. L. *Biophys. J.* **1990**, *58*, 533–548.
(31) Rao, S. N.; Kollman, P. *Biopolymers* **1990**, *29*, 517–532.
(32) Hausheer, F. H.; Singh, U. C.; Palmer, T. C.; Saxe, J. D. *J. Am. Chem. Soc.* **1990**, *112*, 9468–9474.

were observed are helix bends and kinks, non-Calladine rule behavior, some unusual torsional angles, and nonplanarity in the base-pair orientations resembling those observed in A-DNA. An MD simulation based on the GROMOS force field with explicit water molecules and counterions was also reported,[33] in which the GROMOS force field was augmented by a harmonic restraint function for hydrogen bonds involved in Watson–Crick base pairing to prevent axis deformations and base pair opening. The resulting structure belongs to the B-DNA family with a 2.3 Å rms deviation from the canonical form and is also in good agreement with the X-ray crystal structure of the dodecamer, showing similar local axis deformation and large propeller twist in the base pairs. Removal of the Watson–Crick hydrogen bonding restraint function results in higher amplitude of buckling of the base pair, an expansion of the minor groove and an appearance of a kink in the C3–G4 base step. The structure that results from the simulation with the hydrogen bond restraint shows little agreement with the NMR structure proposed by Nerdal et al.[34] The solution structure derived from NMR is significantly underwound, displays significant kinks at the C3–G4 and A6–T7 base steps, and is clearly not the same as the crystal structure. The kinks appear to be similar to those reported for the *Eco*RI restriction site bound to its endonuclease.[35]

Here we present results from a 150-ps MD simulation study of the dodecamer d(CGCGAATTCGCG)$_2$ based on the AMBER force field with no additional constraints and including counterions and more than 1400 water molecules. The resulting structure is different from that obtained by Swaminathan et al.,[33] but is in better agreement with the NMR structure.[34]

Methods

The energy minimization and molecular dynamics simulations were performed with the program AMBER 3.0,[36] using the standard unmodified all-atom force field parameters for nucleic acids included in the program. Because the system included the DNA, the counterions, and a solvation shell of 9 Å, a cutoff distance for nonbonded interactions of 16 Å was used throughout. Other MD simulations of DNA[33,37] used shorter cutoff distances and employed periodic boundary conditions.

The initial geometry of the dodecamer d(CGCGAATTCGCG)$_2$ was generated using the EDIT module of AMBER, as a standard Arnott right-handed B-DNA.[38] Twenty-two Na^+ cations were placed around DNA at bifurcating positions of the OPO angle at a distance of 5.0 Å from the phosphorus atom. The Na^+ cations were assigned a Lennard-Jones radius of 1.6 Å, a well depth ϵ = 0.05 kcal/mol, and a mass of 22.9 atomic units. To construct the solvent environment, the DNA and the counterions were placed in a cube of "Monte Carlo" TIP3P water. Water molecules with oxygen atom closer than 2.9 Å or farther than 9 Å or with hydrogens closer than 2.1 Å or farther than 9 Å from any solute atoms (DNA + counterions) were discarded. This placed 1431 water molecules around DNA. No boundary conditions were applied.

At these initial conditions the system represents approximately 0.03 M solution of DNA in water. Because of the fixed ratio of counterions to DNA, the concentrations of sodium counterions is 22 times the concentration of DNA, which corresponds approximately to 0.7 M.

The initial energy minimization was performed in two steps. The minimization was first restricted only to the positions of water molecules. The partial minimization was followed by an optimization of the entire system, DNA and water. The steepest descent method was used during the first 100 steps of minimization and was followed by the conjugate gradient method. The convergence of the minimization was set at a value of 0.1 for the rms gradient.

The minimized structure was used as an initial geometry for the MD simulations. The MD simulation used a constant temperature algorithm with a bath temperature of 300 K and a coupling parameter τ of 0.2 ps. The SHAKE constraint, which keeps specified bonds frozen, was used for all bonds that involved hydrogen atoms. During the simulation, a time step of 0.001 ps was used; the matrix of nonbonded interactions was updated after every 0.020 ps of simulation.

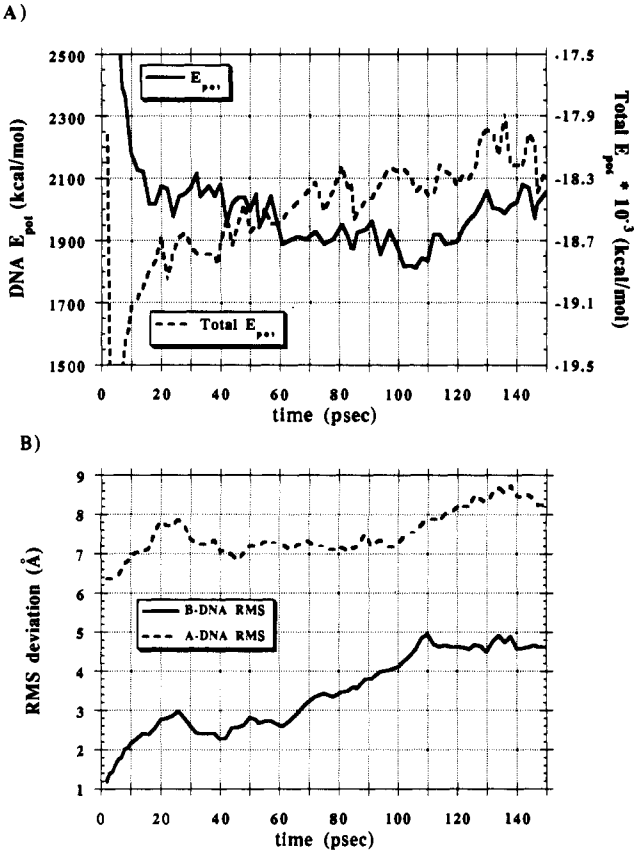

Figure 1. Variations of potential energy of DNA and the rms deviation of the DNA in the course of the dynamics simulation. (A) Potential energy of DNA (—) and total potential energy (--). (B) Two rms deviation curves are shown: one with respect to a standard B-DNA and the other with respect to a standard A-DNA structure.

The first 2.2 ps of the dynamics were used for the equilibration of the system and for the removal of residual steric strain after the minimization. Eleven 0.2 ps runs at 300 K were done for this purpose, each of which started with velocities assigned from a Maxwell distribution at 50 K additionally scaled by 0.001. The remaining parameters were as described before. Following the equilibration runs, the velocities were reassigned once more from a Maxwell distribution and the 150-ps production run started. We found the initial 2.2-ps equilibration stage essential for the stability of the water shell. Without this procedure some water molecules showed a tendency for rapid dissociation from the system.

The structures were stored every 0.1 ps to be used for averaging and further analysis. The analysis of the results from the MD simulation was performed with the MDANAL and ANAL modules of AMBER. The averaged structures were minimized in the same way as described above. The averaged minimized structures were analyzed with the CURVES program.[39]

Results and Discussion

General Characteristics of the Molecular Dynamics Simulation. The total potential energy of the system shows a drift toward higher values in the course of the MD simulation (see Figure 1A). To analyze the reasons for this drift, the total potential energy of the system was divided into contributions from the DNA, the water ensemble, and the counterions (CIO) as well as from the interactions between these groups. The extent of the drift was quantitated by fitting a line to each curve starting at a simulation time of 20 ps. The drift of the total energy reflects mostly the changes in the potential energy of the counterions and much less those of the ensemble of water molecules; the interaction of DNA with water is also contributing to the upward drift. The total

(33) Swaminathan, S.; Ravishanker, G.; Beveridge, D. L. *J. Am. Chem. Soc.* **1991**, *113*, 5027–5040.
(34) Nerdal, W.; Hare, D. R.; Reid, B. R. *Biochemistry* **1989**, *28*, 10008–10021.
(35) McClarin, J. A.; Frederick, C. A.; Wang, B. C.; Green, P.; Boyer, H. W.; Grabel, J.; Rodenberg, J. M. *Science* **1986**, *234*, 1526.
(36) Singh, U. C.; Weiner, P. K.; Caldwell, J.; Kollman, P. A. *AMBER 3.0*, University of California: San Francisco, CA, 1986.
(37) Hausheer, F. H.; Singh, U. C.; Saxe, J. D.; Flory, J. P.; Tufto, K. B. *J. Am. Chem. Soc.* **1992**, *114*, 5356–5362.
(38) Arnott, S.; Hukins, D. W. L. *J. Mol. Biol.* **1973**, *81*, 93–105.
(39) Lavery, R.; Sklenar, H. *J. Biomol. Struct. Dyn.* **1988**, *6*, 63–91.

Table I. Mean and rms Deviation (in Parentheses) of Structural Parameters Averaged for Three Time Intervals

	20–60 ps	100–150 ps	B-DNA[b]	A-DNA[b]
P–P distance (Å)	6.90 (0.23)	6.95 (0.25)	6.46	5.64
helical repeat angle (deg)	38.5 (3.3)	32.6 (3.5)	34.2	29.9
		34.5 (3.5)[a]		
sugar pucker phase angle (deg)	111.8 (43.6)	140.3 (53.5)	191.3	13.1
	$^1_0$T	$^2_1$T	C3′-exo	C2′-endo
backbone torsional angles (deg)				
α	261.8 (35.2)	207.3 (46.8)	313.2	276.1
β	158.7 (18.6)	176.8 (19.6)	214.0	207.9
γ	77.7 (21.7)	127.3 (29.1)	36.4	45.5
δ	135.5 (12.5)	139.4 (15.4)	156.4	84.3
ϵ	233.3 (26.1)	247.0 (17.2)	155.0	179.5
ζ	221.9 (29.0)	213.9 (22.6)	264.9	310.9
χ_{pur}	248.7 (15.4)	254.2 (17.4)	262.2	205.8
χ_{pyr}	253.2 (16.6)	262.9 (19.0)	262.0	205.8

[a] Excluding the first residue which has repeat angle of 15°. [b] Values for A- and B-DNA structures generated by AMBER.

potential energy of the DNA (see Figure 1A) is decreasing very slowly; the interaction of the counterions with the DNA and the water has a much bigger contribution to the time dependent stabilization of the system.

The potential energy of DNA decreases rapidly during the first 20 ps, but subsequently the rate of the change is on the average only −1.5 kcal/ps. Consequently, DNA structures before this time point, i.e., 20 ps, were not considered in the structural analysis. A closer examination of the potential energy of DNA, Figure 1A, shows a small decrease after 20 ps, with abrupt changes around 60 and 100 ps. These changes in potential energy reflect changes in the structure of DNA, as can be seen from the behavior of the rms during the dynamics simulation (Figure 1B). The rms deviation from the B-DNA structure (see Figure 1B) in the time range 20–60 ps is quite stable around a value of 2.60 ± 0.20 Å. However, starting at 60 ps the rms grows rapidly and reaches 4.64 Å around 100 ps. After 100 ps the rms deviation from B-DNA stabilizes around 4.64 ± 0.16 Å. Figure 1B also displays the rms deviation from the A-DNA structure, which is larger than for B-DNA, with an average value of 7.46 ± 0.60 Å. In contrast to the rms from the B-DNA, the rms deviation from A-DNA remains quite stable during the dynamics simulation showing some time dependent increase only in the 100–120-ps interval. Based on the observed changes in the potential energy and the rms deviation from B-DNA, the dynamics simulation has been divided into three intervals, 20–60, 60–100, and 100–150 ps, and structures of the DNA have been analyzed separately in 20–60 and 100–150-ps time periods, where only fluctuations of DNA around a stable structure have been observed. In the 60–100 ps time interval the structural parameters of DNA have shown continuous changes, and therefore the DNA structure was not analyzed in this interval.

The Structure of DNA. The average structural parameters for the three time regions used in the analysis are displayed in Table I, in comparison to the values for A- and B-DNA. The average values of intrastrand P–P distances, sugar puckering phase angle, and helix repeat angle for all three time intervals are very close to the values for B-DNA. A similar trend is noticeable for the torsional angles β, χ, and δ. Other backbone angles, especially α and γ in the 100–150-ps interval, are outside the range usually found in crystalline DNA structures and they exhibit large variations in the structural parameters along the DNA chain. The angles α and γ are mainly distributed in two conformational regions. One domain of α angle values is around 270° (−sc), i.e., in the region of α angles usually found in crystalline structures; the other domain is around 90° (+sc or +ac). The two regions of α found in the averaged DNA structures correspond to two energy minima for rotation around the P–O bond. However, values in +sc region have been found mostly in nucleotides or dinucleotides. In the crystal structures of double stranded polynucleotides, the values for α angles have been observed mostly

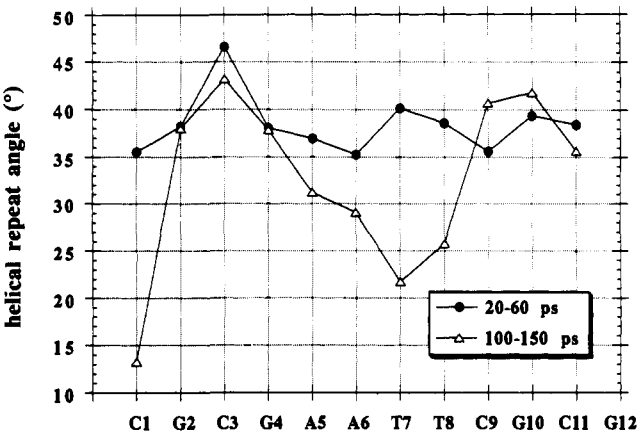

Figure 2. Helical repeat angle along the helix in the two stable simulation intervals: (●) 20–60-ps interval and (Δ) 100–150-ps interval.

Table II. Distribution of Sugar Puckering in the 100–150-ps Interval Displayed as Percentage of Different Pucker States[a]

	C_3'-endo		O_4'-endo		C_2'-endo		O_4'-exo		C_1'-endo		
C1	1	**0**	99	**21**	0	**77**	0	**2**	0	**0**	**C13**
G2	0	**1**	92	**55**	8	**23**	0	**18**	0	**3**	**G14**
C3	2	**7**	98	**70**	0	**14**	0	**5**	0	**4**	**C15**
G4	2	**2**	40	**11**	40	**6**	13	**44**	5	**37**	**G16**
A5	0	**0**	99	**0**	1	**100**	0	**0**	0	**0**	**A17**
A6	24	**33**	58	**5**	6	**1**	4	**6**	8	**55**	**A18**
T7	0	**3**	0	**1**	20	**38**	5	**14**	75	**44**	**T19**
T8	27	**25**	53	**26**	20	**39**	0	**2**	0	**8**	**T20**
C9	16	**5**	21	**85**	39	**6**	10	**2**	14	**2**	**C21**
G10	1	**2**	13	**60**	47	**3**	36	**4**	3	**31**	**G22**
C11	16	**0**	56	**100**	13	**0**	7	**0**	8	**0**	**C23**
G12	0	**0**	10	**7**	3	**15**	21	**53**	66	**25**	**G24**

[a] Left side of each column presents the data for one strand and the right side of each column (in bold face) the data for the complementary strand.

in the −sc domain; however, some exceptional α values have been also observed, such as α = 204° (+ap) found at A5 in crystalline d(CTCTAGAG).[40] Another torsion around the P–O bond, reflected in the angle ζ, shows a similar behavior with two populations in the +sc and −sc domains. The torsional angle around C4′–C5′, γ, also behaves in a bimodal way. The two populations of γ are around 60° (+sc) and around 170° (+ap). The rotation around C4′–C5′ follows a classical 3-fold pattern with minima in the +sc, +ap, and −sc domains. Nucleosides in crystals show values for γ in all three domains, though not with equal populations. In crystalline polynucleotides, however, γ is restricted to the +sc region. The α and γ angles in the averaged DNA structures are anticorrelated by a "crankshaft" motion. Minimia in γ values along the DNA chain correspond to maxima in α values, i.e., α in −sc region corresponds to γ in +sc region, while α in +sc is accompanied by γ in +ap. In the 20–60-ps time interval most of the values of α and γ angles are in −sc and +sc regions, respectively, in agreement with values found in crystal DNAs. However, in the 100–150-ps interval numerous conversions to +sc and +ap conformations are observed. Such conversions between different conformations are reversible, and the averaged change reflects the evolution of the preference for one conformation with time.

The evolution of the helical repeat angle for base pair duplexes shown in Figure 2 is consistent with the structural changes described above. In the 20–60-ps interval the values oscillate around 38°, with a maximum of 46° observed at the C3–G22 base pair. However, in the 100–150-ps time period very substantial unwinding is observed in the central AATT region, resulting in a repeat angle of only 20° at the T7–A18 base pair. The unwinding

(40) Hunter, W. N.; D'Estaintot, B. L.; Kennard, O. *Biochemistry* **1989**, *28*, 2444–2451.

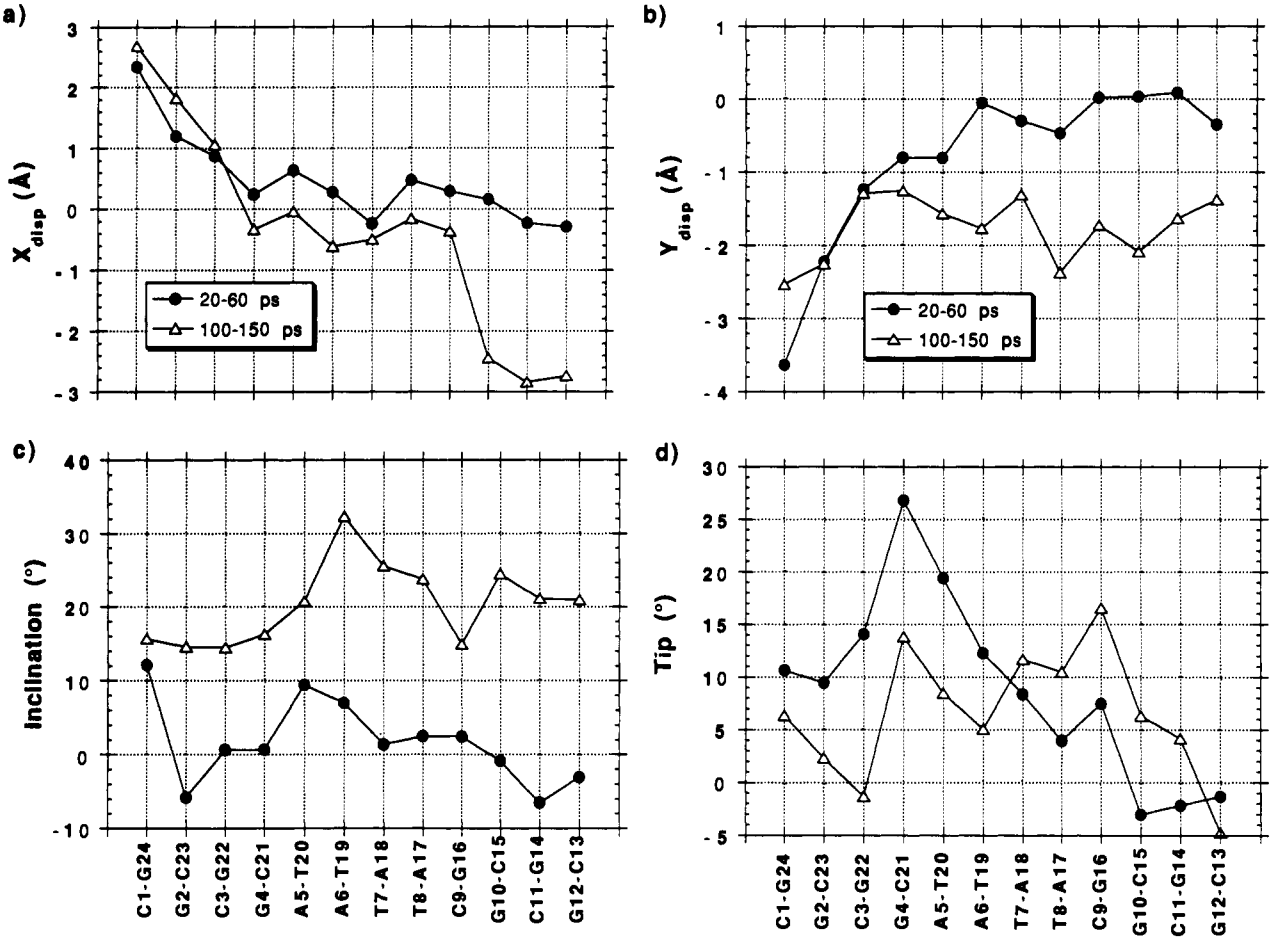

Figure 3. Global base pair–axis parameters in the two stable simulation intervals (●) 20–60-ps interval and (Δ) 100–150-ps interval. X_{disp} and Y_{disp} describe the displacement of the base pair with respect to the global helical axis. Inclination and Tip describe the rotation of the base pair around the y and x directions of the global helical axis, respectively.

observed at the end of the helix is probably due to end effects.

Sugar puckering shows a diversity similar to the backbone torsional angles. Table II shows the percentage population of different sugar pucker states in the 100–150-ps interval. Some sugar moieties have a high conformational stability during the dynamics simulation. For example, C1, C3, A5, and C23 reside most of the time in the O_4'-endo state, while A17 is 100% of the time in the C_2'-endo conformation. The O_4'-endo conformation dominates the pucker states of the sugars, but there are a few highly populated occurrences of C_2'-endo, and C_1'-endo. The high population of O_4'-endo is consistent with experimental results[41] as well as with other MD simulations of DNA.[25,26,29,31] In the crystal structure of this dodecamer, the O_4'-endo conformation was found at C3, T7, and C15.[2] Finally, O_4'-endo has also been found as a favored conformation in an NMR study of d-$(ACATCGATGT)_2$[41] and of the dodecamer simulated in this work.[34] That a relatively high contribution of C_1'-endo is observed for T7 (77%) and the complimentary A18 (55%) may be a result of the local unwinding of the DNA helix, as demonstraed by the small helical repeat angle in this region (ca. 25°). Two important differences exist between the simulated structure and the one derived from NMR.[34] The simulation produces an asymmetric mean structure, whereas the NMR shows a structure with inversion symmetry. Also, C_1'-endo and O_4'-exo pucker conformation of sugars is not observed in NMR, except in unusually substituted sugars.

Analysis of the structural parameters of the DNA was performed with the program CURVES.[39] Global base pair–axis parameters, which characterize the orientation of base pairs with respect to the helix axes, are shown in Figure 3. Total displacement of a base pair can be obtained as $(X_{disp}^2 + Y_{disp}^2)^{1/2}$. In the 20–60-ps interval the first three base pairs are highly displaced away from the axis, whereas the displacement of the rest of the base pairs is small and does not exceed 1 Å. These values are closer to those observed in B-DNA, in which the displacement of base pairs from the helix axis is 0.7 Å, than in A-DNA, where the value is 5.85 Å. In the 100–150-ps interval the displacements are bigger and increase progressively along the C1–G12 direction of the DNA chain. The displacement near the end of the helix (C10–G12 fragment) are almost as high as in A-DNA. The local distortions of the base pair planes are illustrated by the inclination and tip angles, which show that the base pairs are not perpendicular to the axis.

Global base–base parameters, shown in Figure 4, describe the properties of the Watson–Crick base pairs. The shear, stretch, and stagger parameters show the relative displacement of the bases with respect to each other, while buckle, propeller twist, and opening describe the relative orientation of the bases. The distortions increase in the course of the simulation (100–150-ps interval), with the major ones observed in the shear of the C–G base pairs, both C3–G22 and C9–G16. Large distortions are also observed in the propeller twist and opening angles of these base pairs, suggesting that the hydrogen bonding may be disrupted. The analysis of hydrogen bonding is shown in Figure 5. The vertical bars represent the observed mean (center), maximum (top), and minimum (bottom) range of the distances between the hydrogen bonded atoms. Clearly, the major disruption of the hydrogen bonding is in the same C–G base pairs in which the base–base parameters showed considerable deviations. Thus, the pattern of hydrogen bonding disruption and the distortion of base pairs are consistent. The range of the distances between the atoms in which the hydrogen bonds were disrupted is very large, from 3 to almost 9 Å (Figure 5) suggesting that the bases are very

(41) Chary, K. V. R.; Modi, S.; Hosur, R. V.; Govil, G. *Biochemistry* **1989**, *28*, 5240–5249.

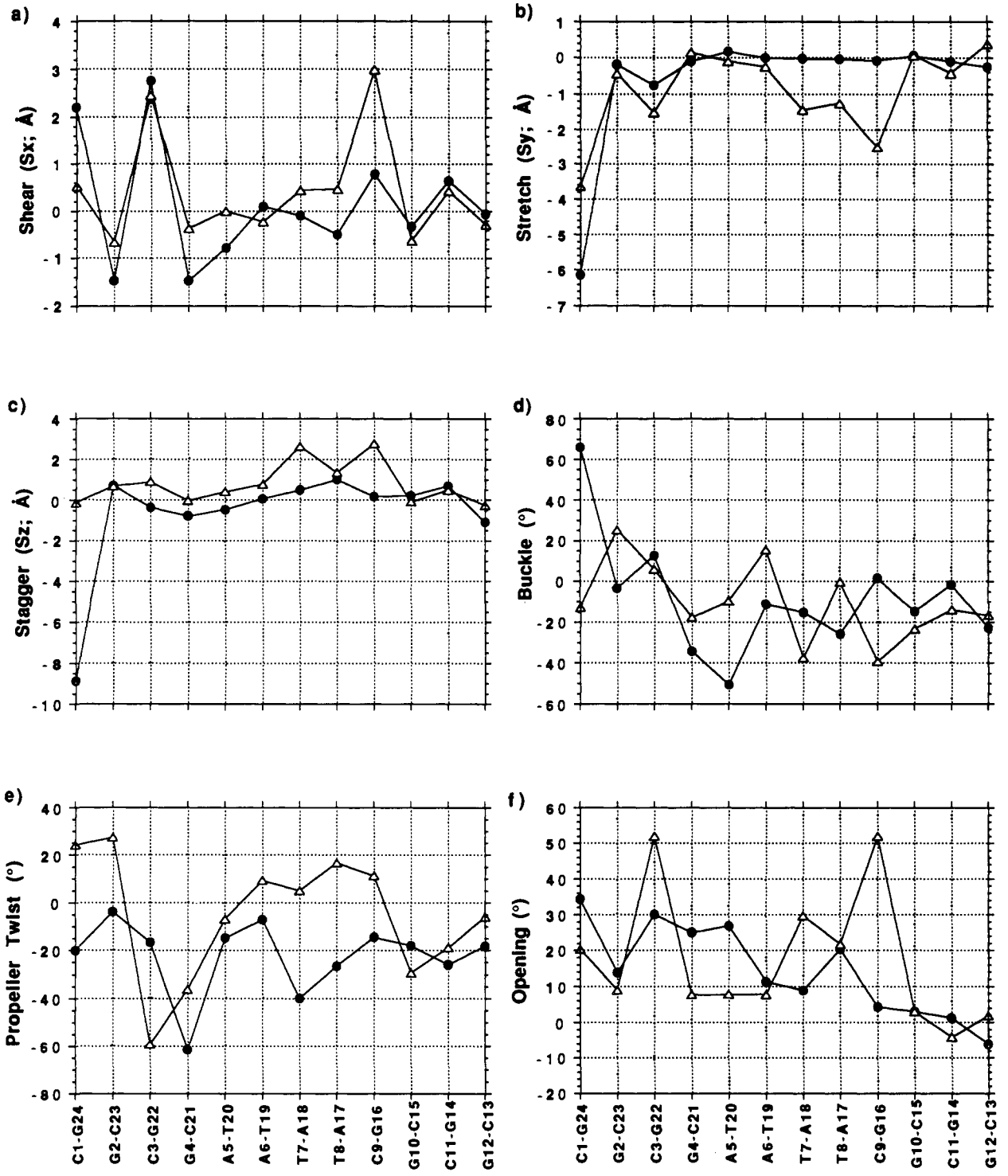

Figure 4. Global base–base parameters in the two stable simulation intervals: (●) 20–60-ps interval and (Δ) 100–150-ps interval.

mobile without hydrogen bonding. On the other hand, the small range of the distances of the hydrogen-bonded bases suggests a much smaller mobility.

Global interbase parameters are shown in Figure 6. The shift, slide, and rise describe displacements of the bases with respect to each other, whereas tilt, roll, and twist indicate the angular relations between them. These parameters are therefore a measure of interbase stacking. Data in Figure 6 indicate that distortions are also observed in base stacking, with especially large values in the 100–150-ps interval. It has been shown that the rigidity of the polynucleotide backbone is enhanced in the presence of base stacking.[42] In unstacked regions of DNA the backbone can be very flexible as indicated by deviation from a regular structure. Thus, the observed distortions in stacking can help explain the increased flexibility of backbone and the presence of some unusual values of the backbone torsional angles discussed above. A schematic summary of the distortions at the bases is illustrated graphically in Figure 7.

The development of the overall distortion of the DNA structure in the course of the MD simulation can be seen in Figure 8 showing the selected structures of DNA. The distortion of the curvature of the helical axis can be expressed by a parameter called shortening, which is obtained from the difference between the sum of path lengths (local fragments of helical axis) and the distance along a straight line that connects the first and the last point of the helical axis. The average shortening at the 20–60-ps interval is 7.8%, and it increases to 19.7% in the 100–150-ps interval. The

(42) Evans, F. E.; Sarma, R. H. *Nature* **1976**, *263*, 567–572.

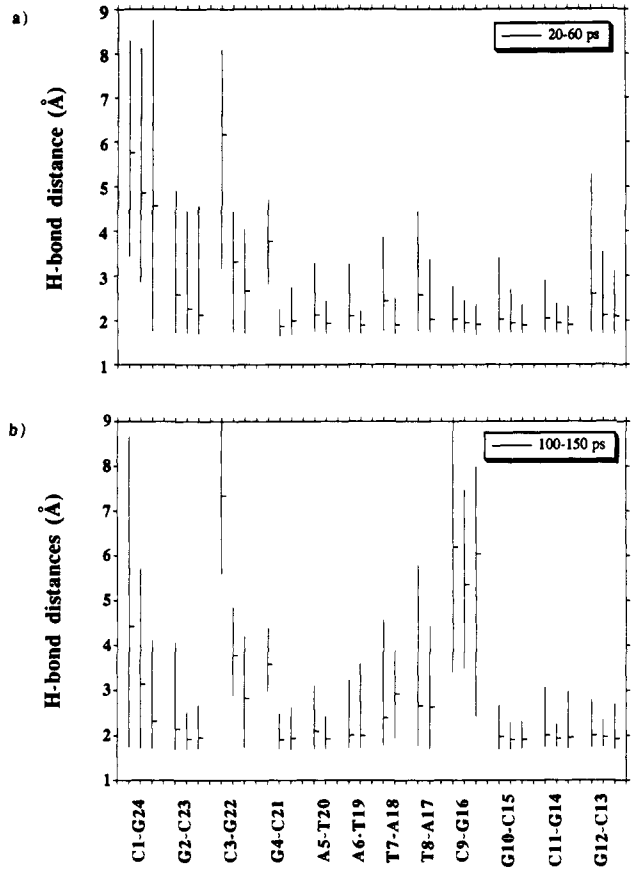

Figure 5. Hydrogen bond distances in the two stable simulation intervals: 20–60-ps interval and 100–150-ps interval. The vertical bars represent the maximum (top), minimum (bottom), and mean (center) distances between the hydrogen bonded atoms.

distortion of the helical axis can also be monitored from the values of the global axis curvature parameters, which measure the displacement and the angular distortion of the axis defined by two consecutive bases. Two very clear kinks develop in the helix near the C3, G4 and C9,G10 as evidenced by high values of the displacement and of the angle formed between local fragments of the helical axis.

A comparison between the structures derived from the NMR data[34] and that obtained from the MD simulation shows only partial agreement. The averaged values of puckering phase angles of C3, G4, A5, A6, and C11 are in the same range as those found in the solution structure of the $d(CGCGAATTCGCG)_2$ determined by Nerdal et al.[34] The phase angles of G2, T7, and G10 determined by NMR are outside the range found in the dynamics with deviations exceeding 100° and those of T8 and C9 show deviations of the order of 50°. The agreement between the glycosylic angles, χ, observed from NMR and from these calculations is only partial. The values published for G2, C3, A5, A6, and T8 are well within the observed values in the MD simulation. The differences in the values for the remaining bases exceed 40°. A comparison of the helical parameters obtained in the simulation to those published[34] shows little agreement. A comparison to the distances observed in the NMR shows a good agreement with those obtained in the simulation (Table III) for intranucleotide distances, but large discrepancies appear for internucleotide distances. Perhaps longer simulation times will be required to explore the structure closer to an equilibrium before such comparisons can become meaningful.

Behavior of Counterions (CIO). The distribution of the Na^+–DNA distances averaged for over 100 configurations covering the time range 2–150 ps is shown in Figure 9. The distribution shows two populations of counterions. The one at distances up to 2.9 Å from the DNA, with a sharp maximum at 2.3 Å, contains approximately 53% of the counterions. The other population is in the rest of the volume, with a flat maximum at 4.25 Å. The

Table III. Comparison between Distances (in Å) Measured by NMR and Derived from the Average Structure Obtained from MD Simulation

interproton distance	NMR[a]	MD simulation
T7-H6/T7-2′H	2.32	2.34 ± 0.48
T7-H6/A6-2″H	2.44	4.67 ± 1.15
T8-H6/T8-2″H	3.70	3.47 ± 0.58
T8-H6/T7-2″H	2.40	3.21 ± 1.13
C11-H6/C11-2′H	2.43	2.30 ± 0.34
C11-H6/C11-1′H	3.59	3.68 ± 0.22
C11-H6/G10-1′H	3.37	4.05 ± 0.54

[a] From ref 34.

maxima correspond to typical locations of counterions near a phosphate group, as illustrated in Figure 10. The structure shown in Figure 10a illustrates a direct coordination between Na^+ and a phosphate oxygen at a distance of 2.3 Å. The Na^+ is also surrounded by five water molecules that complete its first solvation sphere. A short distance of 1.66 Å is observed between one of the water molecules and the other phosphate oxygen. The structure shown in Figure 10b illustrates another type of interaction of counterions with the phosphate, through the solvation sphere. The Na^+ is coordinated by six water molecules and is positioned 4.37 Å away from the phosphate oxygen. Close distances are observed between the phosphate oxygen and two water molecules (1.98 and 1.79 Å), which form a bifurcated hydrogen bonding situation. A small number of cations have also been found far away from DNA in the "bulk" water. Approximately 4% of the counterions can be found beyond the distance of 6 Å from the phosphate in agreement with the long-distance component shown in Figure 9.

Direct coordination of cations to the base atoms in the minor groove has been observed previously. In an ApU crystal one of the two Na^+ ions interacts with the uracil O_2 atom, while the other is coordinated to the phosphate group.[43] In a GpC crystal, on the other hand, both ions are coordinated to the phosphate group.[44] The positions of Cs^+ cations were determined in fiber X-ray study of phage T2 CsDNA.[45] The Cs^+ cations in the major groove are separated from the phosphate groups by water molecules, but in the minor groove the cations are directly coordinated to the O_2(pyr) or N_3(pur) atoms forming bridges of the type: O_2–Cs^+–O_2, O_2–Cs^+–N_3, or N_3–Cs^+–N_3. Such bridges were proposed to play a role in the stabilization of the B-form of DNA.[45] With these experimental observations in mind, all the trajectories generated during the molecular dynamics simulation were searched for structures in which cations interact with base atoms. The only three configurations in which short distances between counterions and base atoms have been observed are shown in Figure 11a–c. All are very minor events because the counterions are mostly found in the neighborhood of the phosphate groups. The structure in Figure 11a shows a potential interaction between a Na^+ cation and a guanine. However, the interaction is not direct but involves the waters of hydration of Na^+. Although it is in the minor groove, the counterion makes no bridging interactions with another base atom of the DNA. The structure shown in Figure 11b is an illustration of the interaction between a counterion and the electron rich double bond of cytosine. The cation is coordinated through a water molecule to the phosphate group and is also close to the C_5–C_6 double bond of cytosine. Although the structure in Figure 11c is a rare event in the dynamics simulation, it is an interesting example of a bridge between the O_4' of the sugar and the N_3 of the adenine base through a counterion and its hydrating water molecules.

Several types of mobility of the counterions have been observed during the MD simulations. Guided by the radial distribution

(43) Seeman, N. C.; Rosenberg, J. M.; Suddath, F. L.; Kim, J. J. P.; Rich, A. J. Mol. Biol. 1976, 104, 109–144.
(44) Rosenberg, J. M.; Seeman, N. C.; Day, R. O.; Rich, A. J. Mol. Biol. 1976, 104, 145–167.
(45) Bartenev, V. N.; Golovamov, E. I.; Kapitonova, K. A.; Mokulskii, M. A.; Volkova, L. I.; Skuratovskii, I. Y. J. Mol. Biol. 1983, 169, 217–234.

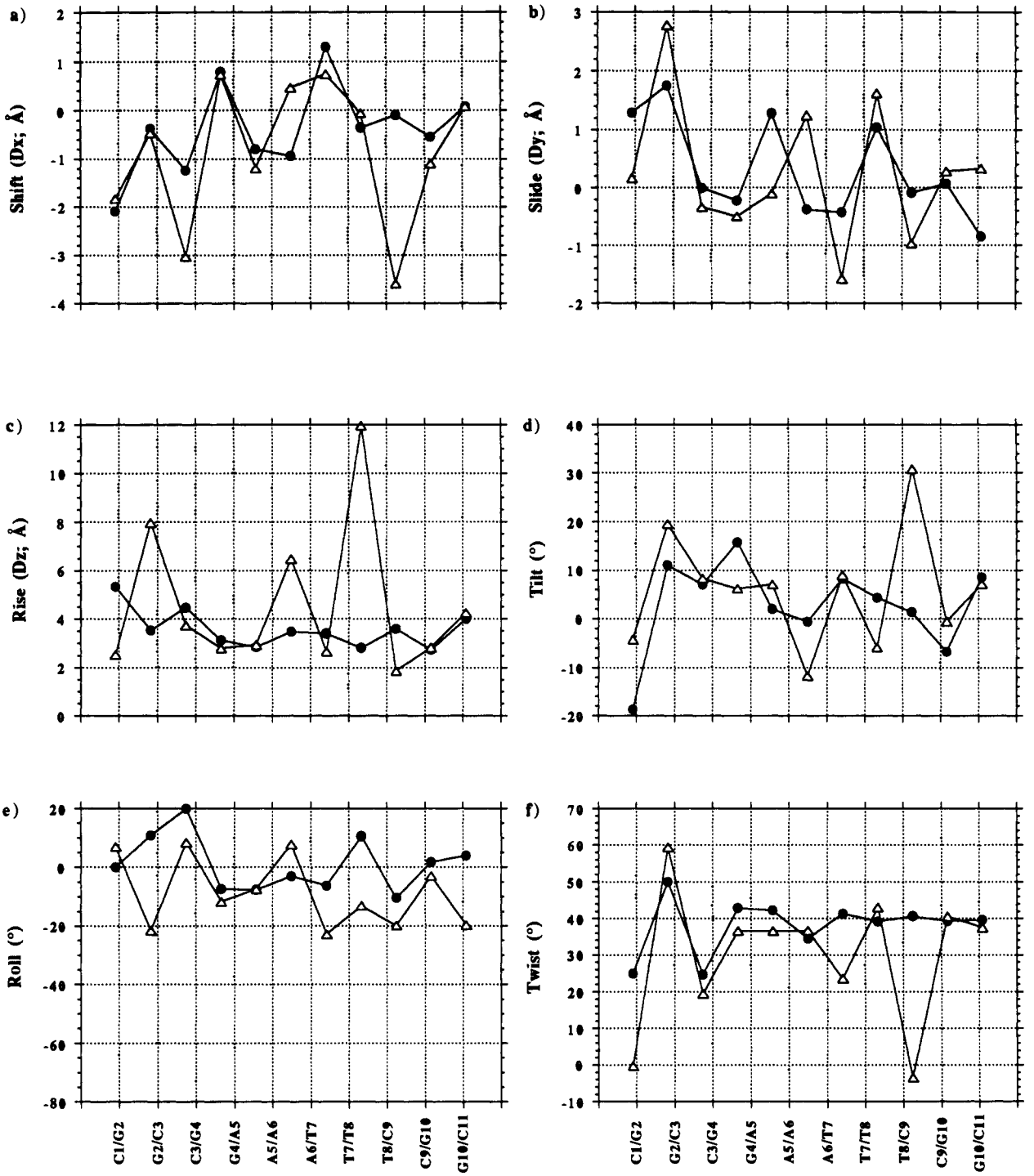

Figure 6. Global interbase parameters in the two stable simulation intervals: (●) 20–60-ps interval and (Δ) 100–150-ps interval.

shown in Figure 10, the counterions were arbitrarily divided into three shells: the direct coordination shell was taken to include all counterions up to 3.0 Å from DNA, the second shell was defined to span the radial distance between 3.0 and 6.0 Å, and the third shell included counterions beyond 6 Å from DNA. In the course of the MD simulation several ions remained in one shell. This behavior is illustrated in Figure 12a for CIO-9 and in Figure 12b for CIO-15. The counterion CIO-9 remains 100% of the time in the first shell at an average distance of 2.42 ± 0.14 Å from P_9, the phosphate that bridges between C_9 and G_{10}. The small standard deviation of the mean distance indicates that in the first shell the counterions perform only small fluctuations around an equilibrium position (see also Figure 12 (parts c and d)). The counterion CIO-15 resides almost all the time in the second shell at an average distance of 3.98 ± 0.76 Å from the DNA. Here the fluctuations are much larger and the counterion also migrates approximately in the 5′ to 3′ direction along the helix axis from P_{16} through A_{17} to the neighborhood of T_{19}. Several counterions show movement from the first coordination shell to the second shell, in which they are totally solvated by water (see Figure 10b), and some proceed into the bulk layer. Such movements are illustrated by CIO-22 shown in Figure 12c and CIO-6 in Figure 12d. The counterion CIO-22 starts in the first shell near P_{23}, moves out into the bulk to reside closer to C_{23}, and then returns to the second shell near the same phosphate, P_{23}. CIO-6, on the other hand, starts in the first shell near P_6 and moves in a perpendicular direction to the helical axis crossing from one strand to the other, ending in the bulk shell, but closest to P_{18}. Overall analysis of the residence time of all the counterions in the three shells shows that on the average they reside approximately equal amounts of time in the first and second shell (ca. 45% of the time in each shell), and only 5% in the bulk. Considering the coun-

Table IV. Average Distribution of Water Around Various Groups of DNA in a Shell of 3 Å[a]

sugar/PO_4		cytosine		guanine		adenine		thymine	
O5′	0.15	N1	0.00	N9	0.00	N9	0.00	N1	0.00
$(CH_2)5'$	1.13	(CH)6	0.39	(CH)8	0.24	(CH)8	0.40	(CH)6	0.21
(CH)4′	0.60	(CH)5	0.65	N7	0.49	N7	0.22	C5	0.00
O1′	0.11			C5	0.00	C5	0.00	$(CH_3)7$	1.58
(CH)1′	0.24	C4	0.01	C6	0.00	C6	0.00	C4	0.00
(CH)3′	0.48	$(NH_2)4$	1.79	O6	0.45	$(NH_2)6$	1.47	O4	0.30
O3′	0.17	N3	0.12	(NH)1	0.10	N1	0.00	(NH)3	0.10
$(CH_2)2'$	0.63	C2	0.00	C2	0.00	(CH)2	0.34	C2	0.00
PO_4	4.13	O2	0.26	$(NH_2)2$	1.52			O2	0.26
				N3	0.08	N3	0.29		
				C4	0.00	C4	0.00		
total	7.65	total	3.22	total	2.88	total	2.71	total	2.45

[a] Average total number of water molecules for a base pair: G–C = 21.38; A–T = 20.45.

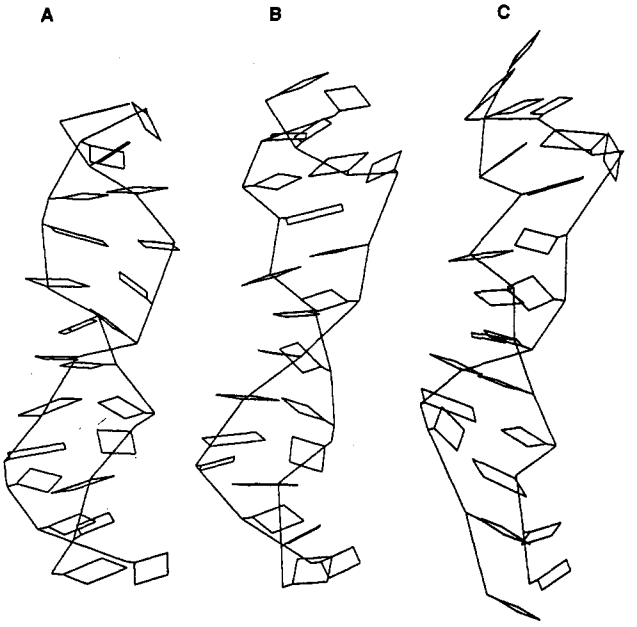

Figure 7. A schematic representation of the development of the overall distortion of the DNA structure in the course of MD simulation. Single frame structures at different time intervals: (A) 32, (B) 72, (C) 142 ps.

terions in the first shell as the only neutralizing species, DNA appears to be approximately 50% dissociated.

Behavior of the Water Layer. Because periodic boundary conditions were not used in this simulation, the structure of the water environment was not studied here in detail. The distribution of water oxygen distances from DNA, shown in Figure 13, is clearly bimodal with the first hydration shell extending to ca. 3.5 Å with a sharp maximum at 2.5 Å. The next shell has a broad distribution with a maximum at about 5.0 Å. The water shell was fairly stable in the course of the MD simulation, as shown in Figure 14. During the MD simulation the water shell expanded continuously, but even after 150 ps more than 80% of the water shell was within the original distance of 9 Å. Only one water molecule completely escaped from the system and was found at a distance of 30 Å from DNA at the end of the dynamics simulation. More importantly, the first hydration shell of DNA remained very stable during the dynamics. About 20% of the water molecules were within 3 Å from DNA during the entire time of the MD simulation. The percentage of water molecules within 6 Å from DNA, i.e., up to the second maximum, changed only very slightly in the course of the simulation; from approximately 60% after equilibration, at the beginning of the dynamics simulation, to about 50% at the end of the run.

The hydration of DNA described as the average number of water molecules near the various atoms of the sugar/phosphate and the bases is shown in Table IV. The main hydration site

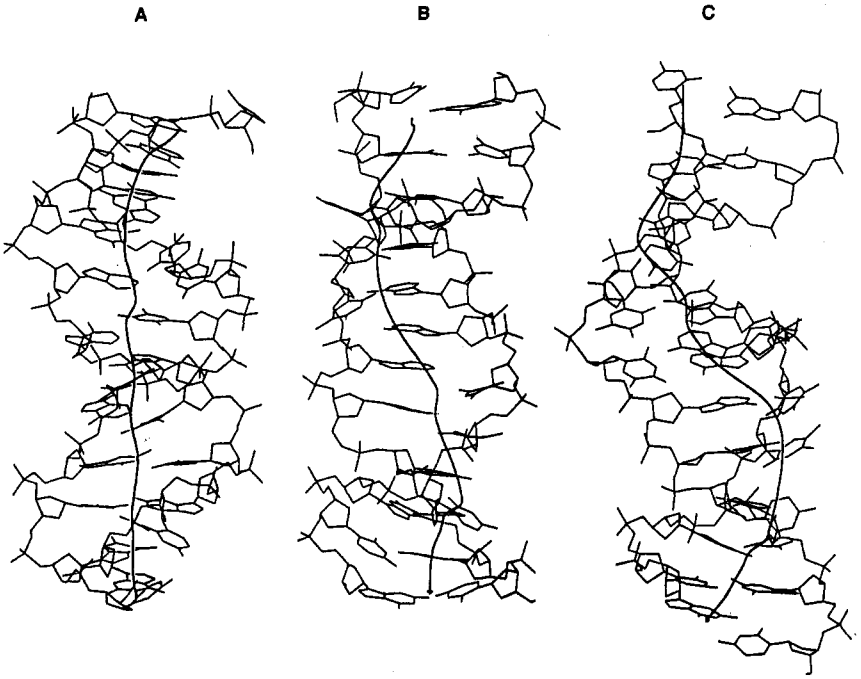

Figure 8. Single frame structures at different time intervals, (A) 32, (B) 72, (C) 142 ps, showing the development of the distortion in the helical axis in the course of the simulation.

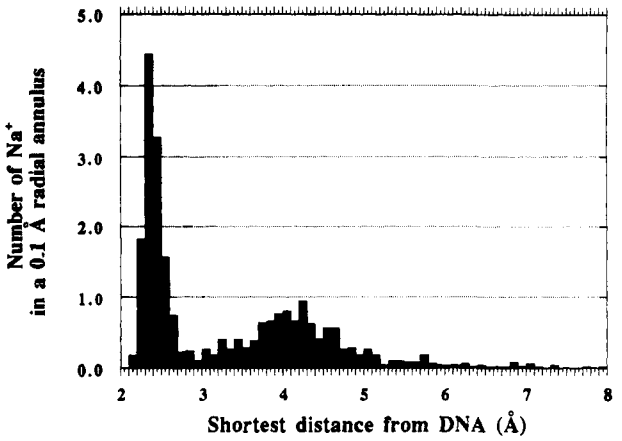

Figure 9. Distribution of average Na^+–DNA distances in the simulation interval from 2 to 150 ps.

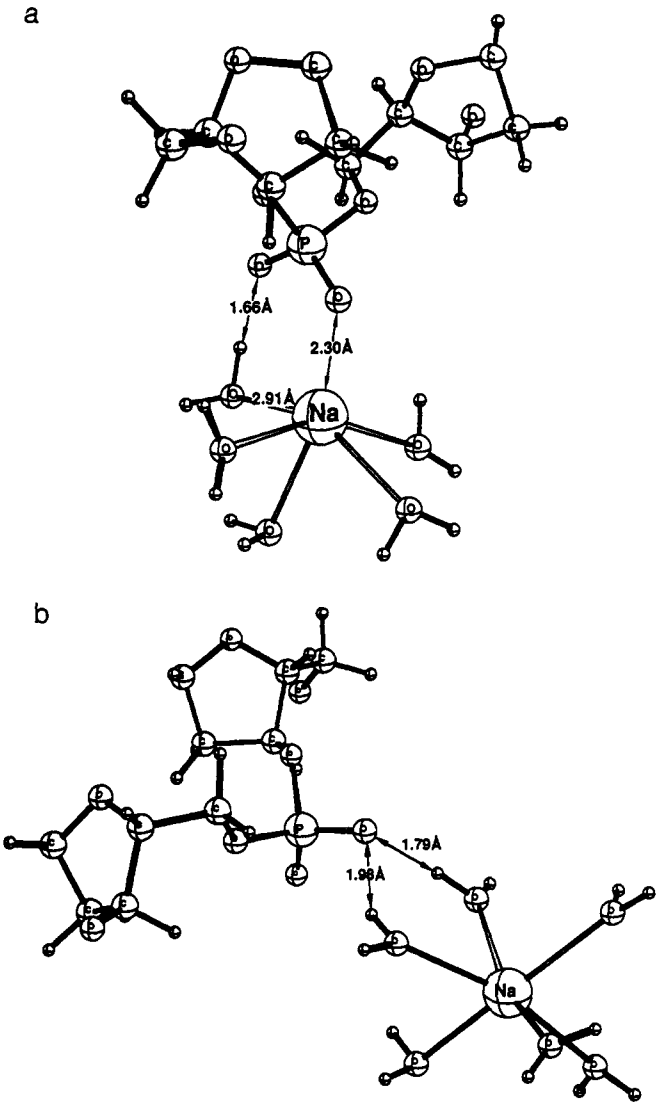

Figure 10. Typical positions of counterions near phosphate groups: (a) an example of direct coordination and (b) an example of coordination through waters of hydration.

in DNA is the phosphate with an average of 4.13 water molecules identified within a distance of 3.0 Å. The next most populated group is the deoxyribose with an average of 3.52 water molecules within 3.0 Å around it. The 5′-CH_2 group is better solvated than the 2′-CH_2 group, indicating that the 2′ position is less accessible to water. The 4′-CH site has on the average 0.60 water molecules around it, which is almost four times as much as around each of the sugar oxygens. This is possibly due to the difference in the

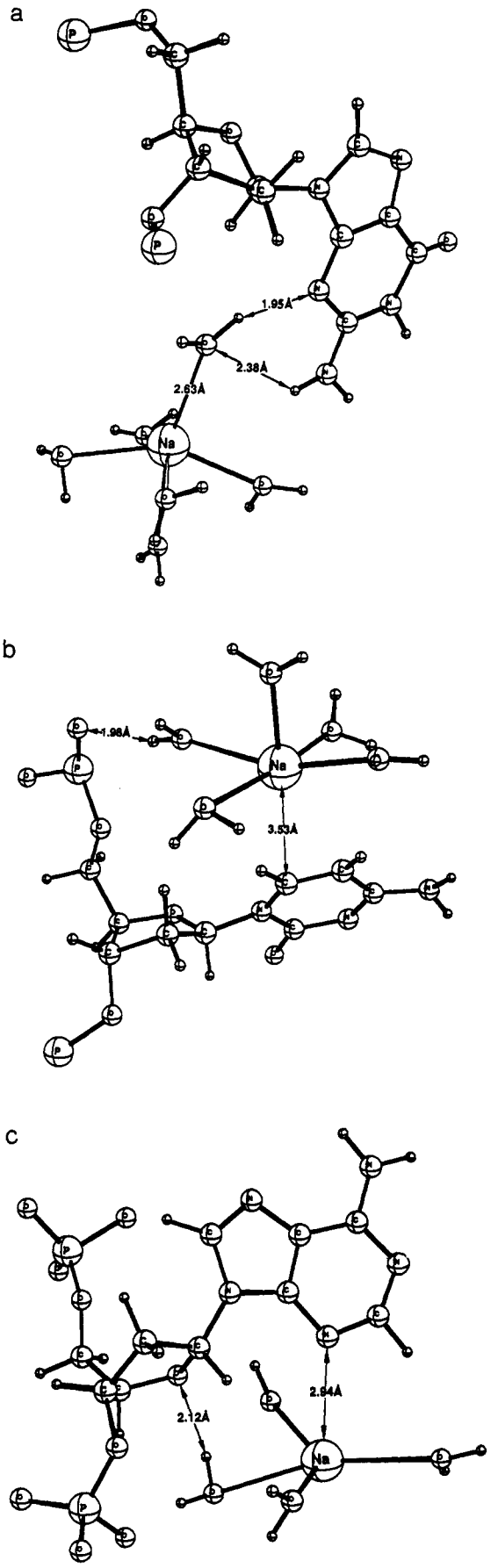

Figure 11. Examples of configurations with counterions in interacting distance from base atoms: (a) interacting with N_3 and NH_2 of guanine through a water molecule, (b) in proximity to C_6 of cytosine; and (c) interacting with N_3 of adenine and with O_1' of deoxyribose through a water molecule.

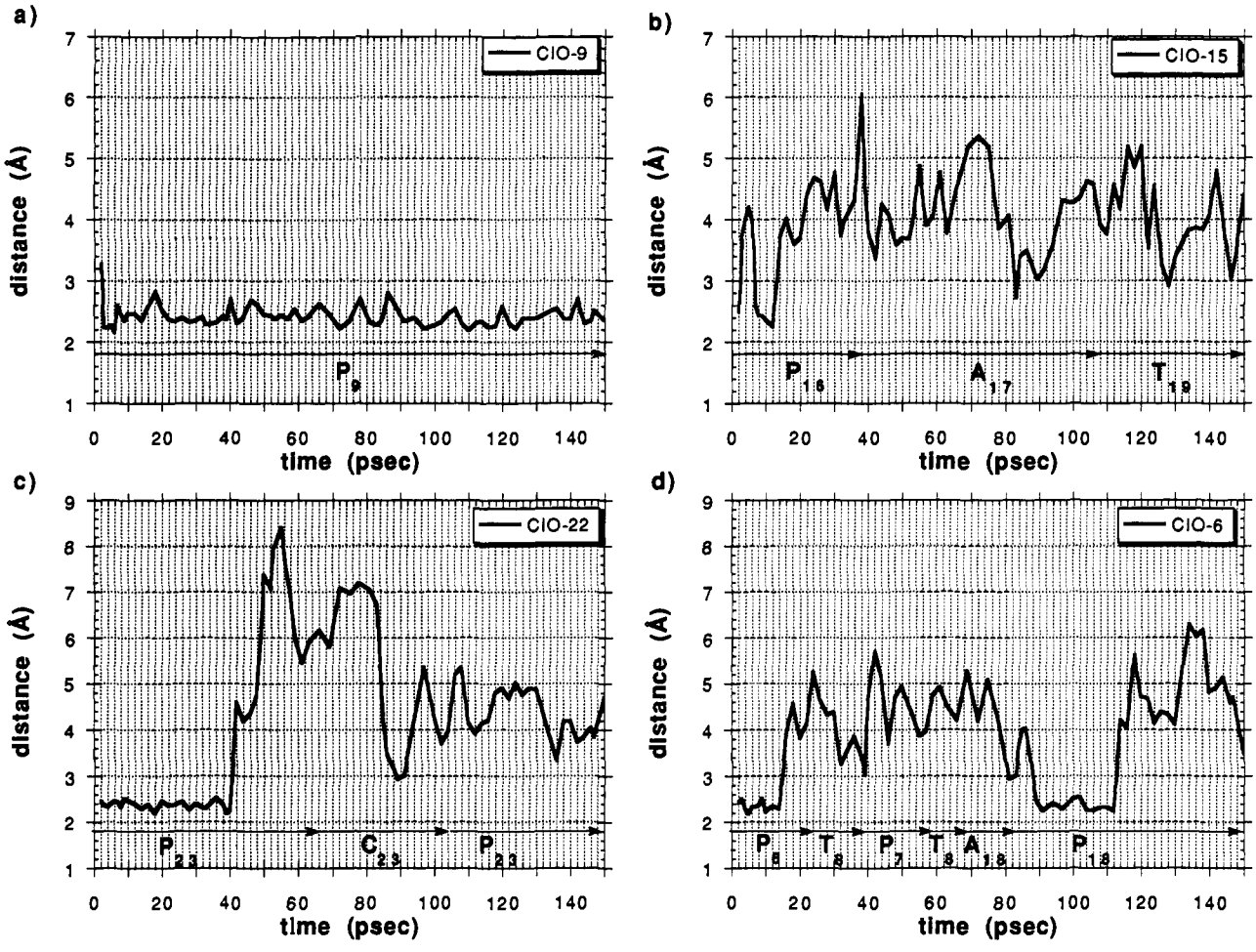

Figure 12. Representative trajectories of four types of counterions described by their distance from the DNA as a function of simulation time.

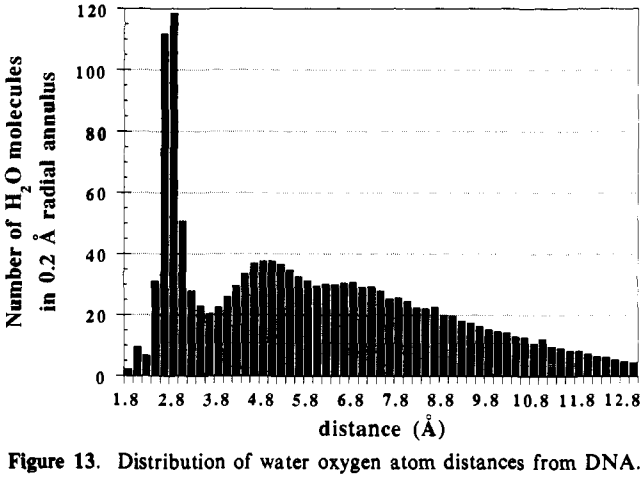

Figure 13. Distribution of water oxygen atom distances from DNA.

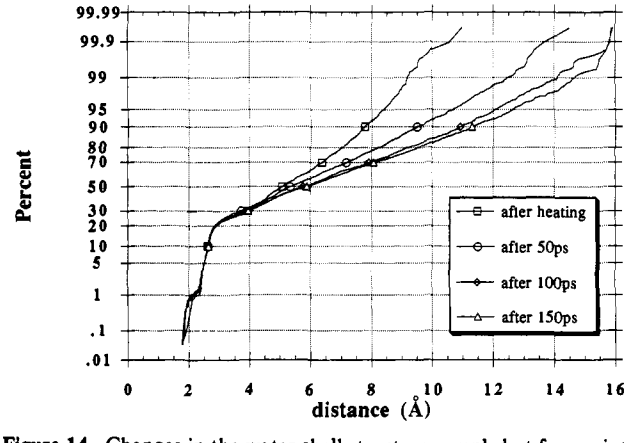

Figure 14. Changes in the water shell structure sampled at four points in the course of simulation. The first solvation shell consisting of approximately 50% of the water molecules remains stable in the course of the simulation.

accessible surface area of a C–H group as compared to an oxygen atom. Among the bases, cytosine is the most hydrated and thymine the least. The G–C base pairs are better solvated, with 21.38 water molecules, than the A–T pairs, with only 20.45 water molecules. The largest number of water molecules can be found on the exocyclic amine groups of the bases; they all average around 1.6 water molecules per NH_2 group, regardless of whether they are located in the minor groove (guanine) or the major groove (cytosine and adenine). The atoms of the bases facing the major groove are usually better solvated than those facing the minor groove. For example, the C_8H and N_7 in the purines and the double bonds on the pyrimidine have more water molecules in their vicinity than the O_2 atoms of the pyrimidines and the N_3 of purines. The observed picture of DNA hydration is in full qualitative agreement with results from experimental and theoretical studies on hydration of DNA.[46-48]

Concluding Remarks

The results of the simulation indicate a high degree of flexibility and mobility in the structure of the DNA and its environment, i.e., water and counterions. The analysis of the various structural parameters shows continuous changes of structure that lead from

(46) Drew, H. R.; Dickerson, R. E. *J. Mol. Biol.* **1981**, *151*, 535–556.
(47) Kopka, M. L.; Fratini, A. V.; Drew, H. R.; Dickerson, R. E. *J. Mol. Biol.* **1983**, *163*, 129–146.
(48) Subramanian, P. S.; Beveridge, D. L. *J. Biomol. Struct. Dyn.* **1989**, *6*, 1093–1122.

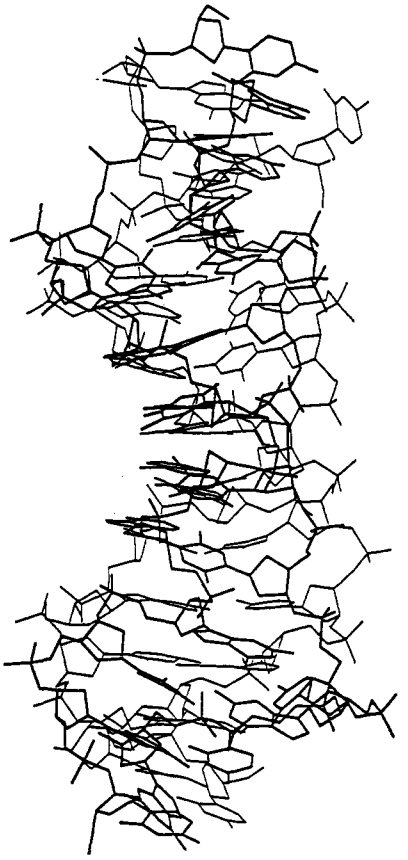

Figure 15. A comparison of two specific frames from the simulation. The energy of the two structures differs only by 0.3 kcal mol^{-1} but the rms deviation between them is 4.2 Å.

an initial B-DNA like structure to one in which the helix is severely distorted and kinked, with disrupted hydrogen bonds between base pairs. Similar disruptions of hydrogen bonding between Watson–Crick base pairs were also observed in the MD simulation by Beveridge et al.,[33] when specific constraints were not applied to the H-bonds.

The results presented here raise the question whether a longer MD simulation would result in a "unique" stable structure of DNA. Such a structure would be the energetic minimum around which the MD simulation would produce limited oscillations. Neither the present results nor the recently published reports[33] provide a definitive answer to this question. Additional experience with simulations performed with a variety of potential functions and boundary conditions and for more extended time periods will be required to approach such insight.

Notably, the theoretical work of Zhurkin et al.[49] suggests that besides the known A- and B-DNA families, several other structures are energetically possible. Their work demonstrates that the DNA is rigid only when the base pairs are fixed, for example, by the interaction of DNA with a protein. However, when the base pairs are allowed to move, different families of structural forms with similar energies can exist with possible continuous interconversions between them. Results from our simulations are compatible with the notion that very different DNA structures may have very similar energies (calculated within the AMBER force field), as is illustrated in Figure 15, which shows two specific frames from the simulation with rms difference of 4.20 Å, but a difference in energies of only 0.3 kcal mol^{-1}. Thus, it seems that a stabilization of a "unique" structure is not supported by the present MD simulations of DNA.

Acknowledgment. This work was supported in part by a grant from the U.S. Department of Energy (DOE), USDOE DE-FG02-88ER60675. H. Weinstein is recipient of a NIDA Research Scientist Award DA-00060. Computations were performed in part at the National MFE Computer Center of the DOE. The authors gratefully acknowledge the generous allocations of computer time at the University Computer Center of the City University of New York, and the Advanced Scientific Computing Laboratory at the Fredrick Cancer Center Research Facility of the National Cancer Institute (Laboratory for Mathematical Biology).

(49) Zhurkin, V. B.; Lysov, Y. P.; Ivanov, V. I. *Biopolymers* **1978**, *17*, 377-412.

Ab Initio Studies of Lipid Model Species. 1. Dimethyl Phosphate and Methyl Propyl Phosphate Anions

Congxin Liang, Carl S. Ewig,* Terry R. Stouch,† and Arnold T. Hagler*

Contribution from BIOSYM Technologies, Inc., 9685 Scranton Road, San Diego, California 92121-2777, and Bristol-Myers Squibb Pharmaceutical Research Institute, P.O. Box 4000, Princeton, New Jersey 08543-4000. *Received August 27, 1992*

Abstract: With the aim of developing force fields for lipid/membrane simulations, extensive ab initio calculations have been carried out on lipid model compounds. This contribution reports results from searching the potential energy surfaces of two simple model species, the dimethyl phosphate and methyl propyl phosphate anions. It is shown that most of the critical structural features of phospholipids found experimentally in crystals, in the gel and liquid crystal phases, and in solution are also seen from quantum mechanical calculations on these simple systems in the gas phase. Thus, a gauche-gauche conformation about phosphate is favored for the dimethyl phosphate anion, as is also seen experimentally for phospholipids (and nucleotides). Also, the COCP torsional angle in the methyl propyl phosphate anion tends to be anti-periplanar or trans, as is the case in most of the structures of phospholipids in crystals and in solution. The vibrational spectra of various conformers of these species have been analyzed in detail. The results reveal some diagnostic frequencies for experimental determination of conformational preferences in structurally related phosphates.

Introduction

Bilayers of discrete lipid molecules, especially the phospholipids, are the primary structural components of both inter- and intracellular membranes in nearly all living organisms and are central to many types of cellular functions such as material transport across membranes and communication between cells. Typically the phospholipids are amphiphilic and consist of a positively charged group plus a phosphate moiety (the α chain) comprising

† Bristol-Myers Squibb.

0002-7863/93/1515-1537$04.00/0